Exploring the halo occupation distribution in nodes and filaments

N.R. Perez[1,2], L.A. Pereyra[3,4], G.V. Coldwell[1,2], F. Rodríguez[3,4] & I.G. Alfaro[3,4]

[1] *Departamento de Geofísica y Astronomía, Facultad de Ciencias Exactas, Físicas y Naturales, UNSJ, Argentina*
[2] *Consejo Nacional de Investigaciones Científicas y Técnicas, Argentina*
[3] *Observatorio Astronómico de Córdoba, UNC, Argentina*
[4] *Instituto de Astronomía Teórica y Experimental, CONICET-UNC, Argentina*

Received: 09 February 2024 / Accepted: 23 April 2024

Resumen / Exploramos la distribución de ocupación del halo (HOD) en nodos y filamentos. Utilizando las simulaciones hidrodinámicas cosmológicas TNG300-1 y el Extractor de Estructuras Persistentes Discretas (DisPerSE), analizamos la HOD en una amplia gama de umbrales de magnitud y colores de galaxias. Nuestros resultados revelan un exceso de galaxias débiles y azules en halos de baja masa en las regiones centrales de los nodos, lo que indica que estas regiones no exhiben el comportamiento de los cúmulos de galaxias virializados. Esto sugiere que la materia continúa acumulándose en estas regiones, afectando sus propiedades dinámicas.

Abstract / We explore the halo occupation distribution (HOD) in nodes and filaments. Using the TNG300-1 cosmological hydrodynamical simulations and the Discrete Persistent Structures Extractor (DisPerSE), we analyse the HOD over a wide range of magnitude thresholds and galaxy colours. Our results reveal an excess of faint and blue galaxies in low-mass halos in the central regions of nodes, indicating that these regions do not exhibit the behaviour of virialised galaxy clusters. This suggests that matter continues to accrete in these regions, affecting their dynamical properties.

Keywords / large-scale structure of universe — galaxies: halos — galaxies: statistics — methods: statistical

1. Introduction

On large scales, galaxies describe a network pattern of nodes, filaments and voids known as the "Cosmic Web" (de Lapparent et al., 1986; Bond et al., 1996). The standard paradigm of the Universe formation suggests that large structures are formed from hierarchical grouping by the continuous accretion of less massive galaxy systems through filaments (Zel'dovich, 1970; Cautun et al., 2014). Then, the filamentary structures play an important role in the properties and galaxy evolution.

Galaxies form and evolve within dark matter halos, so their properties are related to the characteristics of the host halo. Moreover, several papers show the influence of the large-scale environment on galaxy properties such as shape, spin, stellar mass, star formation rate, colour (Tempel et al., 2013; Wang et al., 2020; Lee & Moon, 2023; Einasto et al., 2008; Malavasi et al., 2017; Kraljic et al., 2018; Laigle et al., 2018). The halo occupation distribution (HOD, Peacock & Smith (2000); Berlind & Weinberg (2002); Berlind et al. (2003); Zheng et al. (2005)) links galaxies and dark matter halos by the probability distribution that a halo of mass M contains N galaxies with specific properties.

We emphasise that our aim in this paper is to identify any differences in HODs for different cosmic structures, considering a wide range of magnitude thresholds and galaxy colours.

2. Data and sample selection

2.1. IllustrisTNG

The current analysis is based on the cosmological hydrodynamic simulations, IllustrisTNG* (Marinacci et al., 2018; Naiman et al., 2018; Nelson et al., 2018; Pillepich et al., 2018b,a; Springel et al., 2018), in particular TNG300-1, as it is the most suitable simulation to study the large-scale structure due to its high resolution. Cosmological parameters in the simulation agree with Planck 2015 results (Planck Collaboration et al., 2016): $\Omega_{m,0} = 0.3089$, $\Omega_{\Lambda,0} = 0.6911$, $\Omega_{b,0} = 0.0486$, $h = 0.6774$, $n_s = 0.9667$ and $\sigma_8 = 0.8159$. The simulation employs $2\,500^3$ dark matter particles and $2\,500^3$ gas cells with masses of 5.9×10^7 $M_\odot$ and 1.1×10^7 $M_\odot$, respectively, within a box of 205 h^{-1} Mpc.

2.2. DisPerSE

DisPerSE** (Discrete Persistent Structures Extractor) (Sousbie, 2011; Sousbie et al., 2011; Sousbie, 2013) is a multiscale structure identifier that is based on the discrete Morse theory. This theory applies mathematical properties describing the relationship between the topology and the geometry of the density field to characterise

*https://www.tng-project.org/
**http://www2.iap.fr/users/sousbie/web/html/index888d.html?archive

✉ *Contact* / noeliarocioperez@gmail.com

the Cosmic Web in a mathematical equivalent called the Morse complex.

The filaments and critical point catalogues developed by Duckworth et al. (2020a,b) *** are based on DisPerSE and give the cosmic web distances between each subhalo to the nearest minimum critical point, the nearest 1-saddle point, the nearest 2-saddle point, the nearest maximum critical point and the nearest filament segment. These catalogues are available for 8 snapshots from $z = 0$ to $z = 2$ of TNG300-1 and to build them, the authors selected subhalos with masses higher than $M_* > 10^{8.5}$ $h^{-1} M_\odot$ and set the persistence parameter $\sigma = 4$.

2.3. Sample selection

The sample used in this paper was constructed from the TNG300-1 Groupcat at $z = 0$ snapshot by selecting subhalos with $M_* > 10^{8.5}$ $h^{-1} M_\odot$ in accordance with the filament catalogue. Moreover, the selected subhalos must be contained in halos with masses $M_{200} \geq 10^{11}$ $h^{-1} M_\odot$ (being M_{200} the mass enclosed within a region that encompasses 200 times the critical density) in order to obtain halos with about 10^3 particles.

We obtained for each halo, the distance to the node, the ID of the closest filament and its properties, such as the distance to the axis of the filament. We built different subsamples taking into account the distances and considering halos belonging to nodes and filaments separately. We define nodes with varying radii ($d_n < 0.5, 1.0, 1.5$ and 2Mpc). The filaments are defined with varying widths ($d_f \leq 0.5, 1.0, 1.5$ and 2Mpc) and distances to the nodes ($d_n \geq 0.5, 1.0, 1.5$ and 2Mpc) to exclude halos within nodes. Here, d_n represents the distance to the node and d_f the distance to the filament axis.

3. Analysis

In this section, we explore and compare the HOD for the node and filament samples. To obtain these distributions, we compute the mean number of galaxies per halo mass bins $\langle N_{gal}|M_{halo}\rangle$ and we consider different ranges of absolute magnitudes and colours, in order to study their luminosity and galaxy population dependence. In this sense, we consider the r-magnitude thresholds: $M_r - 5\log_{10}(h) \leq -17, -18, -19$ and -20 and the mean colour value $M_g - M_r = 0.56$ to separate blue and red galaxies. The error bars were calculated using jackknife technique (Quenouille, 1949; Tukey, 1958).

4. Results

It aimed to study how satellite galaxies behave in the halo occupation, following Alfaro et al. (2020); Perez et al. (2024), we calculate the HOD for different absolute magnitude limits (Fig. 1). For the sake of simplicity, only the results for the extreme magnitude limits are presented.

***https://github.com/illustristng/disperse_TNG

For the node samples, the main difference in the HOD between the subsamples occurs for halos with masses lower than 10^{13} $h^{-1} M_\odot$, being this signal stronger for nodes with 1 Mpc radius and decreasing for larger nodes. This finding is strongly related with the absolute magnitude limits, with a higher fraction for weaker magnitudes. The distributions for halos with masses greater than 10^{13} $h^{-1} M_\odot$ are comparable. The HOD for filament subsamples are very similar for halo masses lower than 10^{13} $h^{-1} M_\odot$. However, for higher masses we observed a slight difference, with the halo occupancy being lower for the sample with $d_f \leq 2$Mpc and $d_n \geq 2$Mpc.

To analyse the dependence of the halo occupation with the evolution of stellar populations of the galaxies, we compute the HOD considering the mean value of the $M_g - M_r$ subhalo colours. In Fig. 2, we observed that for the node subsamples, the distributions differ significantly for low-mass halos, while for the higher mass halos the distributions are indistinguishable. These differences are significantly stronger for the blue subhalos respect to the red ones. The HODs for the filament subsamples show an opposite behaviour, being similar for halos with lower masses and clearly differentiated for that with higher masses. This feature becomes more evident for the blue subhalos.

5. Conclusions

We have calculated the HOD for Groupcat at $z = 0$ of IllustrisTNG by selecting halos in nodes and filaments separately. Considering the distances to the nodes and the filament axis provided by the Cosmic Web Distances catalogue, we defined various node and filament subsamples. To identify potential variations in halo occupancy based on galaxy characteristics, we separate galaxies by luminosity and colour.

The node samples show an excess of faint galaxies in halos with masses below 10^{13} $h^{-1} M_\odot$, which decreases for brighter galaxies. This excess is higher for halos closest to the node centre ($d_n < 0.5$Mpc). The occupancy of galaxies is similar in massive halos, regardless of their luminosity. The filament samples show no significant variation, suggesting that galaxy halo occupancy does not appear to depend strongly on filament definition or galaxy magnitude.

Regarding the red sample, the HODs do not depend on the definition used for nodes and filaments, as they overlap. In the node samples an excess of blue galaxies is observed in low-mass halos, while in the filament samples the differences occur within the error bars for massive halos.

The occupancy of the halos in the filaments seems to be similar to that of the halos in the total sample. The excess of faint and blue galaxies in halos with masses lower than 10^{13} $h^{-1} M_\odot$ located in the central regions of the nodes, which would indicate that these regions do not behave like virialized galaxy clusters, probably because the matter is continually falling into these regions.

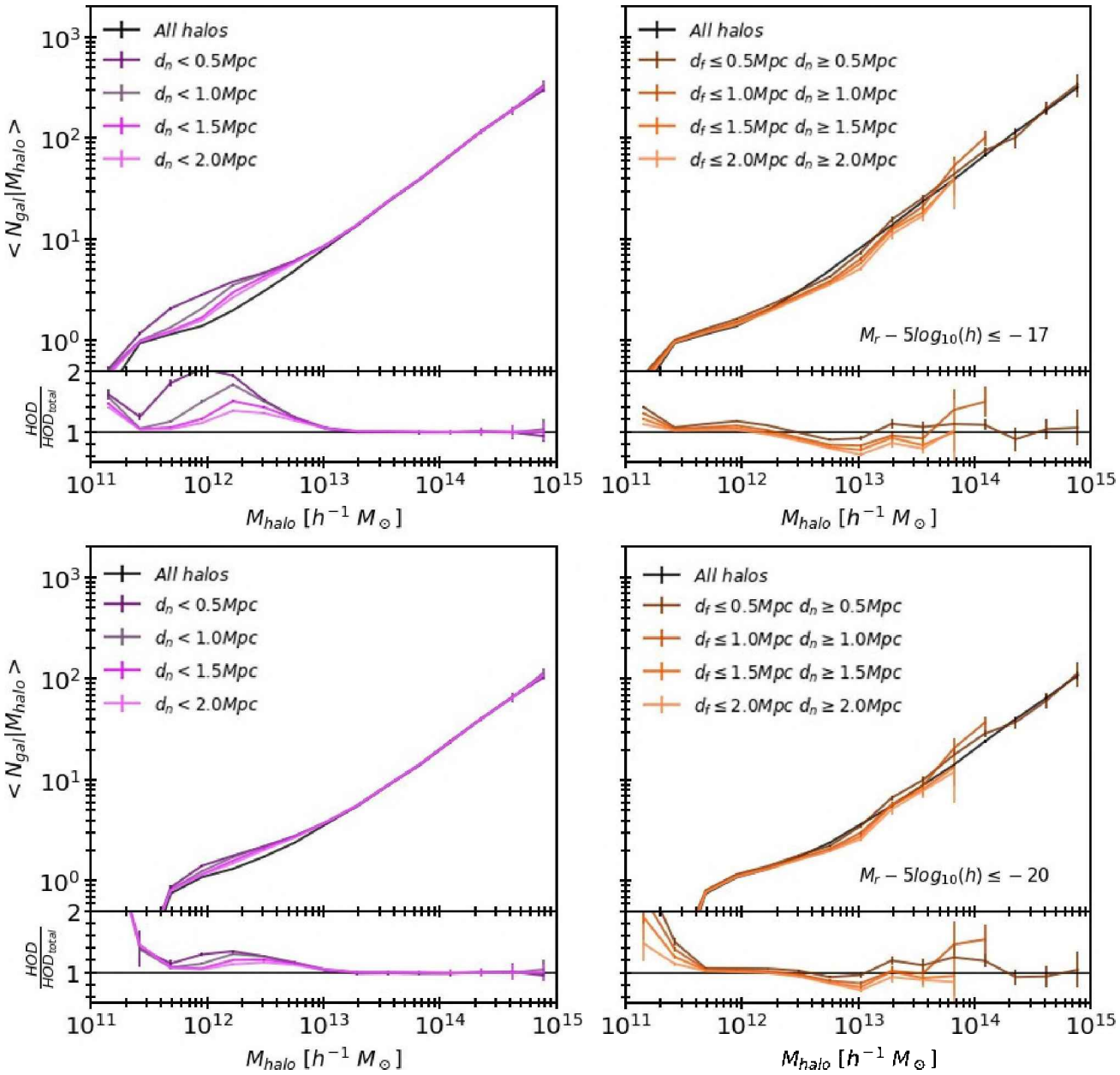

Fig. 1. HOD for the node (*left panels*) and filament (*right panels*) subsamples. The black lines represent the overall HOD for the corresponding limit in magnitude and the coloured lines describe the HOD for different node and filament subsamples. Below each panel we show the ratio between the subsamples and the overall HOD.

Acknowledgements: We thank the referee, for providing us with helpful comments and suggestions that improved this paper. This work was supported by the Consejo Nacional de Investigaciones Científicas y Técnicas de la República Argentina (CONICET). The authors would like to thank the Scientific Committee for giving them the opportunity to present this work at the RAAA65.

References

Alfaro I.G., et al., 2020, A&A, 638, A60
Berlind A.A., Weinberg D.H., 2002, ApJ, 575, 587
Berlind A.A., et al., 2003, ApJ, 593, 1
Bond J.R., Kofman L., Pogosyan D., 1996, Nature, 380, 603
Cautun M., et al., 2014, MNRAS, 441, 2923
de Lapparent V., Geller M.J., Huchra J.P., 1986, ApJL, 302, L1
Duckworth C., Tojeiro R., Kraljic K., 2020a, MNRAS, 492, 1869
Duckworth C., et al., 2020b, MNRAS, 495, 4542
Einasto M., et al., 2008, ApJ, 685, 83
Kraljic K., et al., 2018, MNRAS, 474, 547
Laigle C., et al., 2018, MNRAS, 474, 5437
Lee J., Moon J.S., 2023, arXiv e-prints, arXiv:2305.04409
Malavasi N., et al., 2017, MNRAS, 465, 3817
Marinacci F., et al., 2018, MNRAS, 480, 5113
Naiman J.P., et al., 2018, MNRAS, 477, 1206
Nelson D., et al., 2018, MNRAS, 475, 624
Peacock J.A., Smith R.E., 2000, MNRAS, 318, 1144
Perez N.R., et al., 2024, MNRAS, 528, 3186

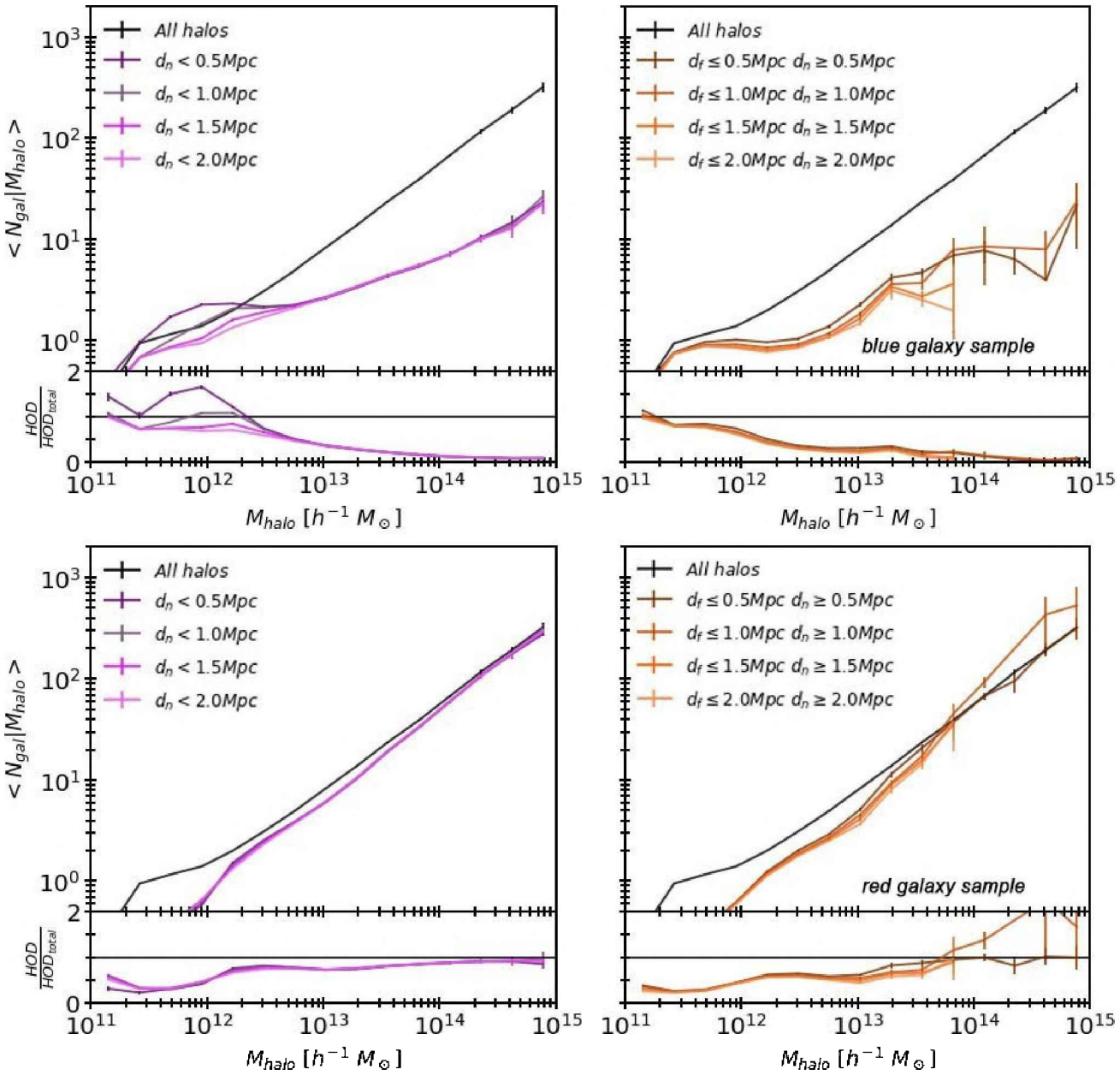

Fig. 2. HOD for the node (*left panels*) and filament (*right panels*) subsamples considering subhalos bluer and redder than the mean value for the whole galaxy population. The black lines represent the overall HOD for the corresponding colour, and the coloured lines describe the HOD for different subsamples of nodes and filaments. Below each panel we show the ratio between the subsamples and the overall HOD.

Pillepich A., et al., 2018a, MNRAS, 475, 648
Pillepich A., et al., 2018b, MNRAS, 473, 4077
Planck Collaboration, et al., 2016, A&A, 594, A13
Quenouille M.H., 1949, The Annals of Mathematical Statistics, 20, 355
Sousbie T., 2011, MNRAS, 414, 350
Sousbie T., 2013, DisPerSE: Discrete Persistent Structures Extractor, Astrophysics Source Code Library, record ascl:1302.015
Sousbie T., Pichon C., Kawahara H., 2011, MNRAS, 414, 384
Springel V., et al., 2018, MNRAS, 475, 676
Tempel E., Stoica R.S., Saar E., 2013, MNRAS, 428, 1827
Tukey J.W., 1958, The Annals of Mathematical Statistics, 29, 614
Wang P., et al., 2020, ApJ, 900, 129
Zel'dovich Y.B., 1970, A&A, 5, 84
Zheng Z., et al., 2005, ApJ, 633, 791